Lunar Reconnaissance Orbiter Wide Angle Camera Photometry: An Empirical Solution. A. K. Boyd, M. S. Robinson, and H. Sato, School of Earth and Space Exploration, Arizona State University, (ABoyd@ser.asu.edu)

Introduction: Other lunar missions employed empirical photometric fits and some have used different photometric functions for mare and highlands [1]. We are deriving one photometric function for the whole equatorial region of the Moon.

The Lunar Reconnaissance Orbiter (LRO) Wide Angle Camera (WAC) in 7-band color mode has a field-of-view (FOV) of 60°, resulting in ±30° emission angle across each line of an image. Such large changes in viewing geometry present challenges to photometric normalization, which is required for mosaicking and sensible color analysis. For example, the ratio of the 689 nm and 321 nm bands has a standard deviation less than 3% in the highlands and ~ 7% globally. The small differences in color mean that errors in the photometric fit will significantly degrade color analyses.

The Moon revolves under LRO once every ~28 days, and the WAC is imaging almost continuously over illuminated terrain capturing a nearly complete mosaic each month [2]. LRO entered its primary mapping phase on 15 September 2009. Since then, there have been over 28 lunations and data for 28 global mosaics. This large number of global photometrically varying observations provides the means to accurately solve for photometric response on a fine scale. The wide FOV and precise pointing data allow the generation of the Global Lunar DTM 100 m (GLD100) [3] that allows topographic photometric angles to be calculated on a 300 meter baseline.

Method: Roughly 20 months of WAC observations were used in this study, and over 65,000 nadir color mode WAC images were processed for the color mosaic. In order to get a more robust data set the 7-band WAC images were filtered on emission angle, phase angle, and incidence angle; the photometric fit is not well behaved at high emission and incidence angles. Local geometry was calculated using the GLD100 [3], this includes local incidence and emission angles as well as the geographic locations of each pixel.

The 704 sample by 14 line LRO WAC visible image framelets were reduced by averaging 4 samples x 2 lines together after full radiometric calibration was completed. The averaging improved the signal-to-noise ratio, as well as reducing the dataset to a more manageable size for a first iteration mosaic. The 128 sample by 4 line UV framelets were not reduced as they are binned 4x4 on chip.

Each pixel value has a value for I/F, phase angle, incidence angle computed on a sphere, incidence angle computed on the GLD100, emission angle computed on a sphere, emission angle computed on the GLD100, latitude, longitude, and image ID associated with it..

Data were restricted by the position on the focal plane, incidence angle, and phase angle. It was found that the data were not well behaved for the empirical photometric function at the extremes of the FOV (emission greater than 27°), at incidence angles greater than 60°, or at phase angles less than 15°. Thus these data were excluded from the fitting.

The empirical photometric fit was derived from a 15°x15° region centered on 0.5° N latitude and 146.5° E longitude. The calculation consisted of over 42,000,000 data points for each of the two WAC ultraviolet bands, and over 92,000,000 data points for each of the five WAC visible bands.

The WAC I/F prediction function has 15 variables for each band, compared with 10 for each band, and 8 fixed for all bands with the RObotic Lunar Observatory (ROLO)[4].

A least-squares fit was performed for the empirically derived photometric function $P(e_s,e,i,g)$ as a starting value for a minimum search function (eq. 1). A minimum search was then performed around the least squares solution for the minimized solution of the non-linear equation 1.

$$F_{min} = norm\left[1 - \frac{\frac{I}{F}}{P(e_s, e, i, g)}\right]$$

Equation 1: ***Minimum error function****. By dividing the I/F by the photometric function, instead of subtracting, the relative errors at higher incidences (lower absolute I/F) are reduced significantly.*

Once a solution was found and applied to the data, the normalized I/F values were binned by geographic location. Each bin has the median, standard deviation, and count recorded. The median value at each bin is the final mosaic value.

Results: The mapped product is created in simple cylindrical coordinates and has a latitude range of -63° to 63° and longitude 0° to 360°. There is nearly uniform data coverage throughout the mapped area, with the 90° and 270° routine spacecraft maneuver locations having noticeably fewer data.

The average standard deviation at each pixel is less than 5% for all bands. The magnitude of the standard deviation is most likely due to geologic differences within each final mosaic pixel location, not photometric residuals.

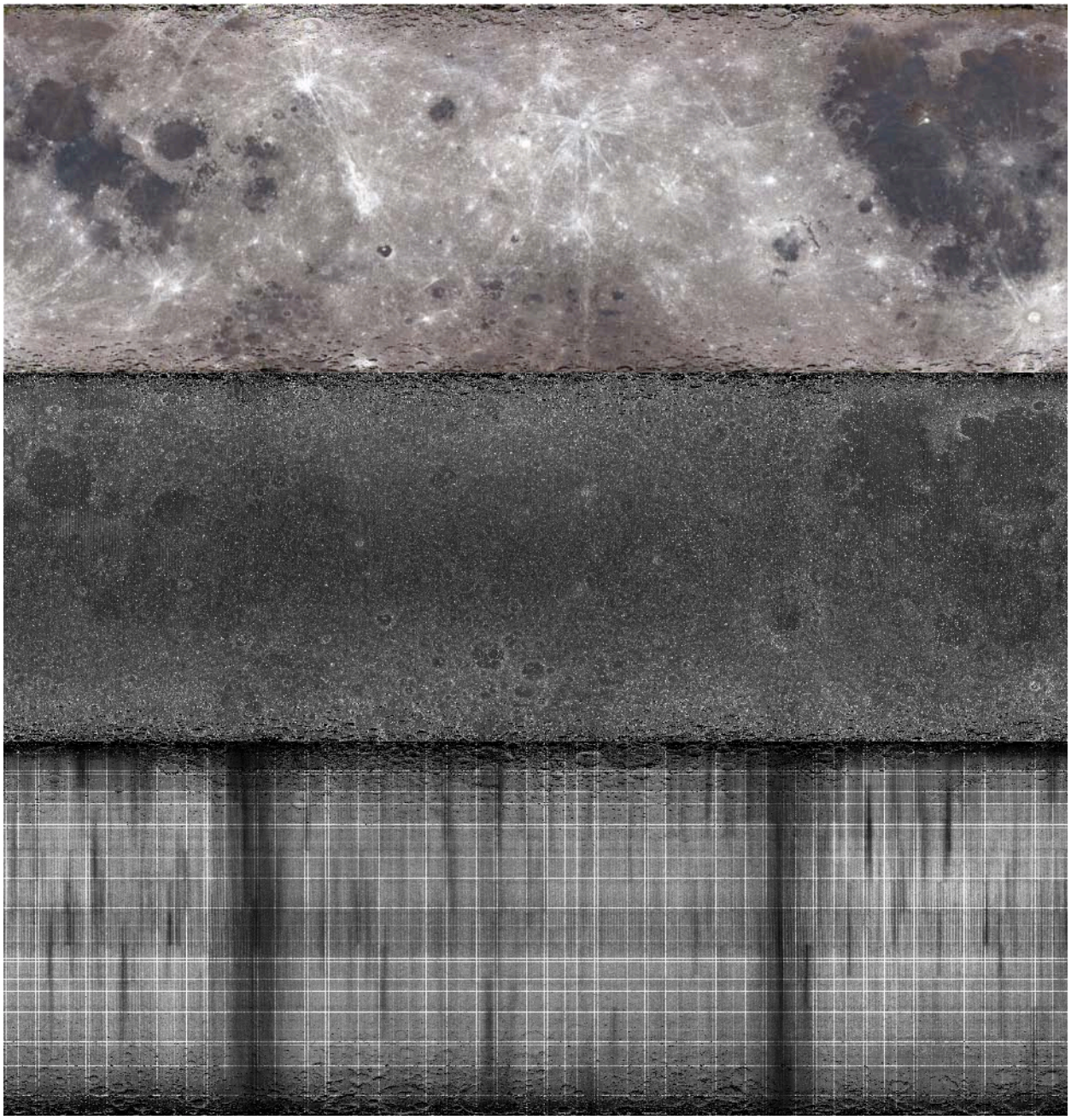

Figure 1. ***Top:*** *R=566 nm G=415 nm B= 321 nm.* ***Middle:*** *Percentage fitting error stretched from 0-20%.* ***Bottom:*** *Number of valid data points stretched from 0 to 200. The very narrow bright bands are areas of duplicate data that occur at file boundaries. The dark bands at 85°E and 265°E are where the momentum dumps and orbit circularization burns occurred during the 50 km mapping orbit. In these regions the average number of data points for each mosaic pixel is roughly 20; the global average is 84 points per pixel. All are equirectangular projections -63° to 63° latitude 0° to 360° longitude.*

References: [1] Hicks et al. (2011) JGR-Planets, VOL. 116, E00G15, 10 PP. [2] Robinson et al. (2010) Instrument Overview [3] Scholten et al. (2012) under review: JGR-Planets. [4] Hugh H. Kieffer and Thomas C. Stone (2005) *The Astronomical Journal* **129** 2887.